

This is a repository copy of *Selective biosorption of Lanthanides onto Galdieria sulphuraria*.

White Rose Research Online URL for this paper:

<https://eprints.whiterose.ac.uk/195432/>

Version: Accepted Version

Article:

Manfredi, C, Amoruso, A J, Ciniglia, C et al. (6 more authors) (2023) Selective biosorption of Lanthanides onto Galdieria sulphuraria. CHEMOSPHERE. 137818. ISSN 0045-6535

<https://doi.org/10.1016/j.chemosphere.2023.137818>

Reuse

This article is distributed under the terms of the Creative Commons Attribution-NonCommercial-NoDerivs (CC BY-NC-ND) licence. This licence only allows you to download this work and share it with others as long as you credit the authors, but you can't change the article in any way or use it commercially. More information and the full terms of the licence here: <https://creativecommons.org/licenses/>

Takedown

If you consider content in White Rose Research Online to be in breach of UK law, please notify us by emailing eprints@whiterose.ac.uk including the URL of the record and the reason for the withdrawal request.

Journal Pre-proof

Selective biosorption of lanthanides onto *Galdieria sulphuraria*

C. Manfredi, A.J. Amoruso, C. Ciniglia, M. Iovinella, M. Palmieri, C. Lubritto, A. El Hassanin, S.J. Davis, M. Trifuoggi



PII: S0045-6535(23)00084-X

DOI: <https://doi.org/10.1016/j.chemosphere.2023.137818>

Reference: CHEM 137818

To appear in: *ECSN*

Received Date: 13 October 2022

Revised Date: 7 January 2023

Accepted Date: 10 January 2023

Please cite this article as: Manfredi, C., Amoruso, A.J., Ciniglia, C., Iovinella, M., Palmieri, M., Lubritto, C., El Hassanin, A., Davis, S.J., Trifuoggi, M., Selective biosorption of lanthanides onto *Galdieria sulphuraria*, *Chemosphere* (2023), doi: <https://doi.org/10.1016/j.chemosphere.2023.137818>.

This is a PDF file of an article that has undergone enhancements after acceptance, such as the addition of a cover page and metadata, and formatting for readability, but it is not yet the definitive version of record. This version will undergo additional copyediting, typesetting and review before it is published in its final form, but we are providing this version to give early visibility of the article. Please note that, during the production process, errors may be discovered which could affect the content, and all legal disclaimers that apply to the journal pertain.

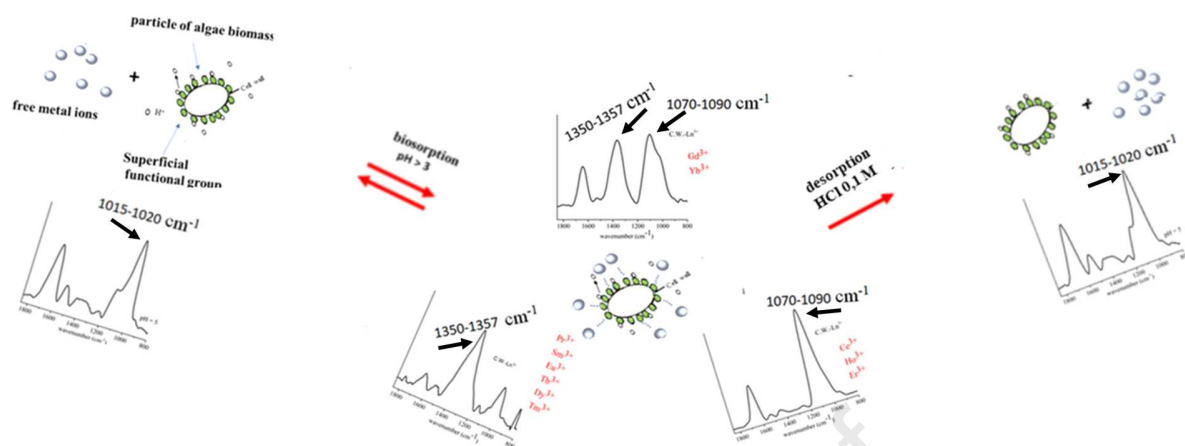
© 2023 Published by Elsevier Ltd.

Author contributions statement

Conceptualization: C.M., C.C; **Methodology:** C.M. **Data curation:** C.M., A.EH; **Resources:** M.T., M.I, S.J.D, M.P., C.C, C.L.; **Investigation:** A.J.A, A. E.H; **Formal analysis:** C.M; **Writing - Original Draft:** C.M,C.C

All authors have read and agreed to the published version of the paper

Journal Pre-proof



Selective biosorption of Lanthanides onto *Galdieria sulphuraria*

C.Manfredi^{a*}, A.J.Amoruso^a, C.Ciniglia^b, M.Iovinella^{b,d}, M. Palmieri^b, C.Lubritto^b, A. El
Hassanin^c, S.J.Davis^{d,e}, M.Trifuoggi^a

^aDepartment of Chemical Sciences, University of Naples Federico II, Via Cintia, I-80126 Naples, Italy.

^b Department of Environmental, Biological and Pharmaceutical Sciences and Technologies, University of
Caserta "L. Vanvitelli", Via Vivaldi 43, 81100 Caserta, Italy;

^cDepartment of Chemical, Materials and Industrial Production Engineering, University of Naples Federico II;

^dDepartment of Biology, University of York, Wentworth Way, York YO10 5DD, UK; mi676@york.ac.uk (M.I.);
seth.davis@york.ac.uk (S.J.D.)

^eState Key Laboratory of Crop Stress Biology, School of Life Sciences, Henan University, Kaifeng 475004, China

E-mail: carla.manfredi@unina.it Tel.: +039
081674379

Fax: +039-081674090

Abstract

The recovering of trivalent Lanthanides from aqueous solutions, by biosorption process onto *Galdieria sulphuraria* lifeless cells, was investigated. Potentiometry, UV-Vis, FTIR-ATR spectroscopy and SEM-EDS analysis were used. All the experiments were performed at 25 °C, in 0.5 M NaCl. Ln³⁺ biosorption is greater in the 5-6 pH range with values ranging from 80 μmol/g to 130 μmol/g (dry weight). The adsorbed Ln³⁺ ions can be recovered at higher acidity (pH<1) and the biosorbent can be reused. Specific molecular interactions between Ln³⁺ ions and the functional groups on *G. sulphuraria* surface were highlighted. Particularly, proteins are involved if Ln³⁺ = Pr³⁺, Sm³⁺, Eu³⁺, Tb³⁺, Dy³⁺, Tm³⁺, while Ce³⁺, Ho³⁺, Er³⁺ form bonds with carbohydrates. Finally, both protein and carbohydrate are involved if Gd³⁺ and Yb³⁺.

A Surface Complexation approach, with a good graphical fitting to potentiometric experimental collected data, was used to describe the biosorption mechanism. This study

34 could be of great applicative utility for removing of trivalent actinides, from waste
35 aqueous solutions, by biosorption. As well known the lanthanides were used
36 as model to simulate the chemical behaviour of actinides in the same oxidation state.

37
38
39 **Keywords:** Lanthanides, *G. sulphuraria*, biosorption, Surface Complexation,
40 FTIR-ATR.
41

42 43 **1. Introduction**

44 Rare earth elements (REEs) are a group of chemical elements including Lanthanides (14
45 chemical elements with atomic number 57-71) and chemically similar elements such as
46 scandium and yttrium. REEs and alloys containing them have a wide variety of high-tech
47 applications such as fluorescent dyes and contrast agents in medical diagnostics and
48 treatments, in wind turbines as permanent magnets, electric car batteries, radar systems,
49 and laser crystals (Chakhmouradian and Wall, 2012; Goodenough et al., 2016; Wall, 2014).

50 That is why they are renamed “vitamins of modern industry”
51 (http://metalpedia.asianmetal.com/metal/rare_earth/application.shtml; Balaram, 2019).

52 The primary sources of REEs are phosphate or carbonate minerals: bastnäsite, monazite,
53 and xenotime and, in near future, the request of yttrium, lanthanum, praseodymium, as well
54 as europium, terbium and dysprosium it may go over the current supply (Balaram, 2019;
55 Kolodynska et al., 2019; Trifuoggi et al., 2017). As well known, the chemical properties of
56 Ln^{3+} are defined by the ionic radius which gradually decreases from lanthanum to lutetium.

57 This makes it difficult to separate them from each other (if held in naturally occurring ores
58 and other mixtures) and very laborious processes are needed. In this context, the main
59 environmental risks during the extraction and processing of REEs are due to radioactivity
60 of radionuclides, such as thorium and uranium, as well as heavy metals (Balassone et al.,
61 2021; Gupta and krishnamurthiy, 2005; Hu et al., 2018; Xie et al., 2014). Biosorption, on

62 the other hand, is a cost-effective method for removing metal ions from aqueous solutions
63 (Kumar et al. 2018, Lucaci et al.2020). Mechanisms, such as passive adsorption, surface
64 complexation, absorption, precipitation and ion exchange, on surface of biological
65 materials (as algae, bacteria, fungi, plants, yeasts ...), determine biosorption. Biosorbent
66 materials must have structural stability, at high acidity, if it is desired to recycle them. The
67 biosorption of metal ions on living cells can be attributed to the interactions with the cell
68 wall (metabolically passive process in few seconds or minutes) and the intracellular ligands
69 (much slower active process involving the transport of metal ions across the cell membrane
70 into the cytoplasm) (Fu and Wang, 2011; Mehta et al., 2016; Michalak et al., 2013).
71 *Galdieria sulphuraria* is a red alga belonging to Cyanidiophyceae, thriving in geothermal
72 sites, at pHs ranging from 0.5 to 5, temperature up to 55°C and in presence of significant
73 amounts of heavy metals, such as arsenic and mercury (Doemel and Brock, 1971). In the
74 last decade, the interest in using *G. sulphuraria* living cells in the bio-uptake of metals
75 grown very rapidly (Fukuda et al., 2018; Iovinella et al., 2022; Ju et al., 2016; Minoda et
76 al., 2015; Sirakov et al., 2021), even supported by the increasingly comprehensive
77 knowledge of their genomes (Ciniglia et al., 2014; Eren et al., 2018).
78 This work was focused on trivalent Lanthanide ions biosorption. The goal was to
79 investigate and understand the interaction mechanisms between *G. sulphuraria* surface and
80 Ln^{3+} . A recent study on living cells of *G. sulphuraria* highlighted that the biosorption of
81 Yttrium, Cerium, Europium and Terbium increases with the pH (Iovinella et al., 2022).
82 These results have suggested a preliminary investigation on the acid-base properties of *G.*
83 *sulphuraria*. Particularly, in this work, the acid-base properties of the functional groups on
84 the surface of *G. sulphuraria* were evaluated in water suspension by potentiometry and
85 Fourier Transform Infrared-Attenuated total reflection (FTIR-ATR) spectroscopy. The
86 interaction properties of *G. sulphuraria* with Ce^{3+} , Pr^{3+} , Sm^{3+} , Eu^{3+} , Gd^{3+} , Tb^{3+} , Dy^{3+} , Yb^{3+}
87 have been investigated by means potentiometry, UV-Vis spectroscopy, FTIR-ATR

88 spectroscopy and Scanning Electron Microscope Energy Dispersive X-ray (SEM-EDS)
89 analysis. All the experiments were performed at 25 °C, in 0.5 M NaCl as ionic medium.
90 Furthermore, the experimental potentiometric data, collected in this work, have been
91 interpreted by using a Surface Complexation Model (SCM) approach, that describes
92 sorption in terms of chemical reactions (similar to aqueous complexation), controlled by
93 thermodynamic, between surface functional groups and dissolved chemical species
94 (Stumm et al., 1970; Huang and Stumm, 1976; Davis and Kent, 1990). SCM, as well
95 known, was used to describe the surface properties and sorption reactions. -

97 **2.Experimental**

99 *2.1. Reagents*

100 Solutions were prepared using double-distilled water and 0.5 M NaCl (as the ionic
101 medium) (Sigma- Sodium chloride puris, p.a., ACS Reagent C 99.5% (AT)). The acid
102 content was determined by a potentiometric-coulometric titration. HCl solutions (Carlo
103 Erba Hydrochloric acid 37% RPE - for analysis – ISO) were standardized by
104 potentiometric-coulometric titrations. All chemicals were commercial.

106 *2.2. Metal stock solutions preparation and standardization*

107 Lanthanide chloride stock solutions were prepared from Ln₂O₃ (Ln³⁺ = Eu³⁺, Er³⁺, Dy³⁺,
108 Ho³⁺, Yb³⁺, 99.99% Aldrich Chemical Co.) and HCl acid. The lanthanide content was
109 determined by EDTA titrations (accuracy of 0.2%), using xylenol orange as indicator.
110 Lanthanide chloride stock solutions were also prepared by dilution of Certipur® Single-
111 Element Standards (1000 mg/L) for Inductively Coupled Plasma Spectroscopy (ICP) by
112 MERK.

115 2.3. *Equipment*

116 Potentiometric measurements, at 25.00 ± 0.03 °C, were conducted in an air thermostat,
 117 measuring the temperature by means a Pt100 TERSID thermocouple. A Hewlett-Packard
 118 (HP) instrumentation was used: an automatic potentiometric data acquisition system and
 119 a HP DC power supply (to perform coulometric titrations). Emf measurements (precision
 120 ± 0.03 mV) of the cell (I)



122 were carried out by using operational amplifiers. The glass electrodes reversible to protons
 123 (*G.E.*) were supplied by Metrohm. A reference electrode (*R.E.*), 0.5 M
 124 NaCl/Hg₂Cl₂/Hg(Pt), placed outside, was electrically connected to the test solution (*TS*)
 125 by means a Wilhelm-type salt bridge. A calibrated resistance coil was connected in series
 126 to the coulometric device (*II*) to measure the potential drop and thus calculate the current
 127 intensity.



130 constant current source

131

132 An external auxiliary electrode (*A.E.*) is a 0.5 M NaCl/HgO_(s)/Hg_(l)(Pt), placed outside,
 133 was electrically connected to the test solution (*TS*) by means a Wilhelm-type salt bridge.
 134 Pt is a platinum electrode.

135 A combined glass electrode (by Metrohm), reversible to free proton, was also used.

136 FTIR-ATR spectra, in the 4000–700 cm⁻¹ range, were recorded on solid phase by Thermo
 137 Nicolet 5700 FT/IR Spectrophotometer using a crystal Zinc Selenide cell. Each spectrum
 138 was recorded 128 times, with spectral resolution 4 cm⁻¹.

139 Absorption spectra, with a Varian Cary 50 UV/Vis spectrophotometer, were recorded
140 using a Quartz Cuvette (10 cm Light Path).

141 Inductively coupled plasma mass (ICP-MS) analysis was carried out by a Bruker Daltonics
142 spectrometer M90 ICP-MS.

143 SEM-EDS analysis was carried out by a Hitachi TM3000 tabletop Scanning Electron
144 Microscope (SEM), equipped with a 15 kV electron beam and an Oxford Instruments
145 SWIFTED3000 EDS probe. High magnification SEM images (5000x) were also acquired
146 using a Secondary Electron source. Energy Dispersive X-ray (EDS) spectra were acquired
147 with the Aztec Energy® software (data collection time 5 min).

148

149 *2.4. Microalgal Culture Preincubation*

150 *G. sulphuraria* strain ACUF 427, collected from the acidic soil of the thermal station in
151 Gunnhver, Southwest Iceland, was taken from the algal collection of the University of
152 Naples “Federico II” (www.acuf.net) (accessed on 20 June 2022). The microalga was
153 cultivated in Allen medium, acidified with H₂SO₄ at pH 1.5, with the following final
154 composition of macroelements: (NH₄)₂SO₄ 24 g/L; K₂HPO₄ 12g/L; KH₂PO₄ 6g/L; NaCl
155 2g/L; MgSO₄(7H₂O) 6g/L; CaCl₂(2H₂O) 0,2g/L; FeSO₄(7H₂O) 0,2g/L; microelements
156 (mg/L): 31 H₃BO₃, 1.25 CuSO₄ · 5H₂O, 22.3 MnSO₄·4H₂O, 0.88 (NH₄)₆Mo₇O₂₄·4H₂O,
157 2.87 ZnSO₄·7H₂O, 1.46 Co(NO₃)₂·6H₂O, 0.014 V₂O₄(SO₄)₃·16H₂O, 0.3Na₂NO₄·7H₂O,
158 1.19 KBr, 0.83 KI, 0.91 CdCl₂, 0.78 NiSO₄, 0.12 CrO₃, 4.74 Al₂(SO₄)₃K₂SO₄·24H₂O (all
159 chemicals were purchased from Sigma Aldrich) in distilled water autoclaved for 20 minutes
160 (Iovinella et al., 2022)

161

162 *2.5. G. sulphuraria biosorbent powder preparation*

163 *G. sulphuraria* biosorbent powders, used in all the experiments performed in this work,
164 were obtained as follows: 500 ml of the microalgal culture (optical density = 5) were

165 centrifuged at 3000g and the resulted pellet was washed twice with ultrapure water at room
 166 temperature. After washing, the pellet into a 2 ml tube was transferred and resuspended in
 167 1 ml of acetone (100% v/v); glass beads were added to the suspension and the tubes
 168 transferred into a Mixer Mill (MM400, Retsch, Gmbh), to perform cell rupture for 5
 169 minutes at maximum speed. Three cycles of cell rupture were performed. Then, cell debris
 170 was suspended in 1 ml 90% DMSO, and homogenized again in Mixer Mill with glass
 171 beads. The tubes were then left shaking overnight at 37°C in a thermostable chamber.
 172 Samples were then centrifuged, the supernatant discarded, the pellet was dissolved in 1ml
 173 100 % Ethanol; 3 more cycles of cell rupture, by adding glass beads were performed as
 174 described above. The final pellet was dried at 37° C.

175

176 2.6. Methodology

177 All the experiments have been conducted on *G. sulphuraria* lifeless cells to ensure
 178 reproducibility of analytical data.

179 Acid–base titrations of aqueous suspensions of *G. sulphuraria* powders, in 0.5 M NaCl, at
 180 25.00 ± 0.03 °C, were performed, by monitoring the emf of the potentiometric cell (I).

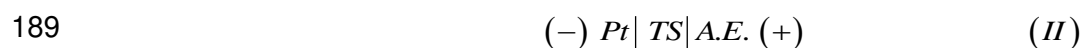


182 Eq. (1) describes the Nernst potential, expressed in mV, of the measuring cell (I).

$$183 \quad E_g = *E_g + 59.16 \log h \quad (1)$$

184 where $*E_g$ is the cell constant, h is free protons concentration at equilibrium. Activity
 185 coefficients are constants in the presence of large concentrations of the medium ions and
 186 thus incorporated in the cell constant (Grenthe, I., 2002). The analytical concentration of
 187 protons was decreased stepwise, by means the auxiliary circuit (II):

188

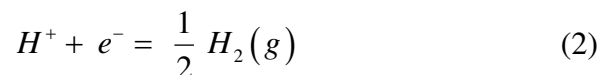


190 constant current source

191

192 Pt is a platinum electrode for the reduction of H⁺:

193



194

The coulometric technique allows for the addition of a precise number of micromoles of electrons without introducing protolytic impurities.

195

196

The microfaradays generated by the circuit (II), Eq. (3), after each supply of current of intensity i (A), for a time t (s), are numerically equal to the number of micromoles of H⁺ reduced on the Pt catode.

197

198

199

$$\mu F = \frac{i \cdot t}{0.096487} \quad (3)$$

200

The equilibrium was assumed to be reached when the potential E_g of cell (I) did not change more than ± 0.03 mV for at least 15 minutes. A potentiometric-coulometric titration of ionic medium was performed to calculate E_g , the potentiometric cell constant, as described in the literature (Gran, 1952; Manfredi et al., 2020).

201

202

203

204

G. sulphuraria suspensions were prepared by resuspending a known amount of biosorbent powders (dry weight ranged from 0.0200 ± 0.0001 g to 0.1200 ± 0.0001 g) in 50.00 ± 0.05 cm³ of 0.5 M NaCl ionic medium. The suspensions were coulometrically titrated by means the circuit (II).

205

206

207

208

The pH range investigated went from 2.5 to 9.

209

210

Acid-base potentiometric titrations of *G. sulphuraria* -Pr³⁺ suspensions, in 0.5 M NaCl, at 25.00 ± 0.03 °C, were also performed, by monitoring the emf of the potentiometric cell (I). The composition of suspensions was as follows: $V = 50.00 \pm 0.05$ cm³, $[Pr^{3+}] = 4 \cdot 10^{-4}$ M, 0.5 M NaCl, *G. sulphuraria* $0,1150 \pm 0.0001$ g (dry weight). The reversibility was ensured throughout the pH range 3 - 7 investigated. The lower limit of acidity was chosen

211

212

213

214 to avoid the precipitation of scarcely soluble oxide of metal ions (Baes and Mesmer, 1977;
215 Biedermann and Sillen, 1953; Ferri et al., 2002; Vasca et al., 2004).

216 Batch biosorption experiments were carried out at pH \approx 5.5. The suspensions were obtained
217 by adding 0.0600 ± 0.0001 g (dry weight) of *G. sulphuraria* biosorbent into 20.00 ± 0.05
218 cm³ of solution with composition: 0.001 M Ln³⁺, 0.5 M NaCl. Suspensions were shaken
219 for 3 hours to achieve adsorption equilibrium, confirmed by the pH stability (\pm 0.01
220 logarithm unit). Lanthanide concentrations, at equilibrium with metal ion biosorbed onto
221 *G. sulphuraria* surface, were evaluated in supernatant by UV-Vis (for Pr³⁺, Sm³⁺, Ho³⁺,
222 Er³⁺) spectrophotometric measurements, or ICP-MS, using the external calibration (or
223 standard addition) method.

224 Desorption experiments, as function of pH, were also conducted. The recovery of Ln³⁺
225 from *G. sulphuraria* -Ln³⁺ samples were resuspended in a known volume (5-10 cm³) of
226 HCl. The pH investigated goes from 0.5 to 2. Suspensions were shaken for 2 hours. The
227 amount of metal ions recovered was evaluate by ICP-MS analysis of supernatant.

228 ATR-FTIR spectra of dried *G. sulphuraria* suspensions, as a function of pH, were
229 recorded. *G. sulphuraria* suspensions were prepared by resuspending a known amount of
230 biosorbent (0.0050 ± 0.0001 g dry weight) in 2 cm³ of 0.5 M NaCl ionic medium at various
231 pH values (pH ranging from 0.5 to 12) for 3 hours. In order to measure the pH, a calibrated
232 combined glass electrode, reversible to free proton, was used. *G. sulphuraria* samples were
233 collected in the form of wet pastes (after centrifugation and remotion of supernatant) and
234 dried at room temperature. ATR-FTIR- spectra of dried *G. sulphuraria* -Ln³⁺ (Ce³⁺, Pr³⁺,
235 Eu³⁺, Gd³⁺, Dy³⁺, Ho³⁺, Er³⁺, Tm³⁺, Yb³⁺) suspensions, obtained by using a similar
236 procedure, were recorded. Particularly, suspensions were prepared by resuspending a
237 known amount of biosorbent (0.0050 ± 0.0001 g dry weight) in 2 cm³ of Lanthanide
238 solution (0.0008 M Ln³⁺, 0.5 M NaCl). All the experiments were repeated 3 times.

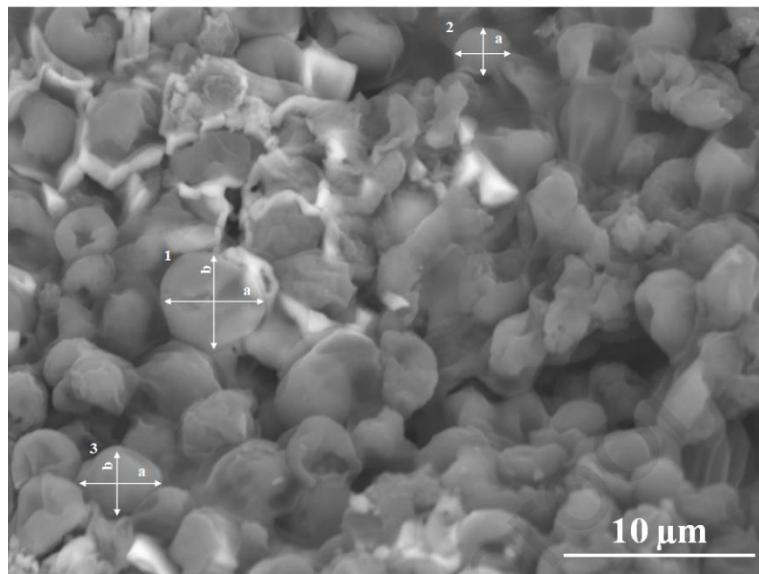
239 SEM-EDS analysis were performed by depositing the dried *G. sulphuraria*-Ln³⁺
240 suspensions (Ln³⁺ = Pr³⁺, Er³⁺, Tm³⁺) on a conductive carbon tape placed on a pin stub.
241 Afterwards, the stubs were sputtered with gold with a Quorum Technologies K650X
242 sputter coater machine (intensity current: 70mA; sputtering time: 750 s; vacuum: 1·10⁻²
243 mbar). High magnification SEM images (5000x) were also acquired using a Secondary
244 Electron source. Images were analysed through ImageJ® program, measuring the size
245 and the ratio between two orthogonal dimensions of the particle (for at least three
246 particles).
247 EDS spectra were acquired with a magnification of 100x, by the Aztec Energy software
248 (data collection time: 300 s).
249

250

3. Results and discussions

251

3.1 Acid-base properties of *G. sulphuraria* in 0.5 M NaCl



252

253

254

Figure 1: SEM image (magnification 5000x) of dried *G. sulphuraria* suspensions in 0.5 M NaCl, pH \approx 5.

255

256

257

Figure 1 shows SEM image, with magnification 5000x, of dried *G. sulphuraria* suspensions (in 0.5 M NaCl, pH \approx 5): the size and the ratio between two orthogonal dimensions of the particle (measured for at least three particles) was \approx 3 μ m and 1, respectively.

258

259

260

261

The number of discrete surface binding sites on the *G. sulphuraria*, the site concentrations and their conditional pKa (valid in 0.5 M NaCl as ionic medium) were evaluated in water suspensions, through potentiometric–coulometric titrations. Primary pH(μ F) data of Figure 2a show that the number of weak acid sites increased with the extent of biomass (the number of micromoles of electrons increases with increasing the biosorbent mass). A good fit of experimental data (dashed lines in Figure 2a) was obtained by assuming two protolytic reactions, Eqs. (4) and (5)

262

263

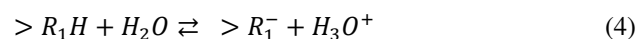
264

265

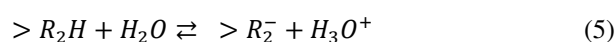
266

267

268



269



270
 271
 272 where R_1 and R_2 indicate two distinct types of acidic groups.

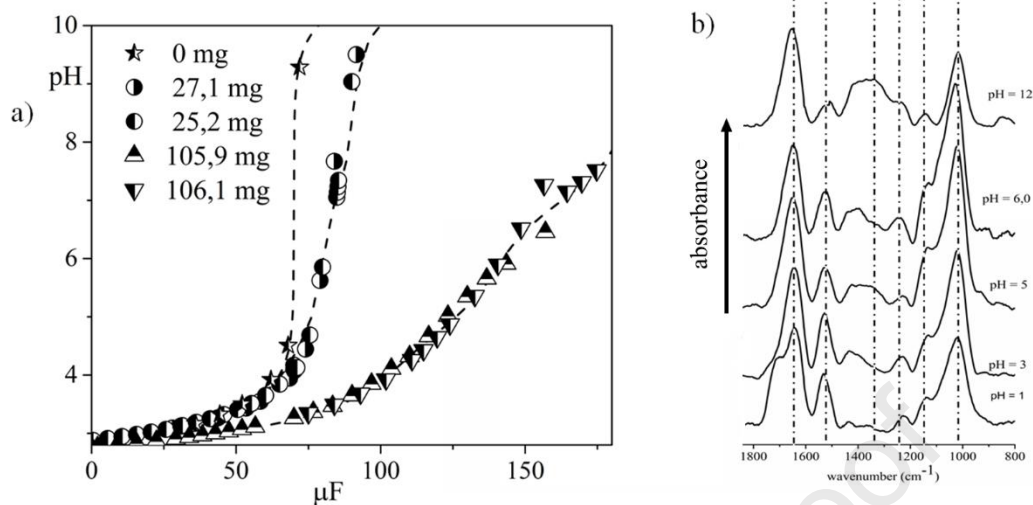
273 Acidity constants, valid in 0.5 M NaCl, and site concentrations (expressed in mmol/g),
 274 calculated by numerical LETAGROP program (Sillen and Warnqvist, 1969), are reported
 275 in Table 1.

276 Table 1: Summary of the equilibrium constants, valid in 0.5 M NaCl, obtained in the
 277 present work, for the *G. sulphuraria*. R_1 and R_2 indicate two distinct types of acidic
 278 groups on surface. The uncertainties (indicated in parenthesis) are to be intended as 3σ .

Sites number (mmol/g, dry weight)	reaction	pKa
0.38(2)	$>R_1H + H_2O \rightleftharpoons >R_1^- + H_3O^+$	4.6(1)
0.43(3)	$>R_2H + H_2O \rightleftharpoons >R_2^- + H_3O^+$	7.0(2)

279
 280 FTIR-ATR spectra of dried *G. sulphuraria* suspensions (in 0.5 M NaCl), as a function of
 281 pH, were recorded. An enlargement of the infrared absorbance spectra, in the 1850–800
 282 cm^{-1} region, is reported in Figure 2b. FTIR peak assignments were based on spectral
 283 values of literature (Barone et al., 2020). Particularly, the most relevant assignments were
 284 as follows: protein Amide I band (mainly $\nu(\text{C}=\text{O})$ stretching, 1640 cm^{-1}); protein Amide
 285 II band (mainly $\delta(\text{N-H})$ bending and $\nu(\text{C-N})$ stretching, $1478\text{-}1575\text{ cm}^{-1}$); proteins
 286 ($\delta(\text{CH}_2)$ and $\delta(\text{CH}_3)$ bending of methyl; $\nu(\text{C-O})$ of COO^- groups, $\delta(\text{N}(\text{CH}_3)_3)$ bending of
 287 methyl, $1380\text{-}1320\text{ cm}^{-1}$); phosphodiester ($>\text{P}=\text{O}$ stretching at $1230\text{-}1240\text{ cm}^{-1}$);
 288 carbohydrates ($\nu(\text{C-O-C})$) in the region $1015\text{-}1020\text{ cm}^{-1}$.

289



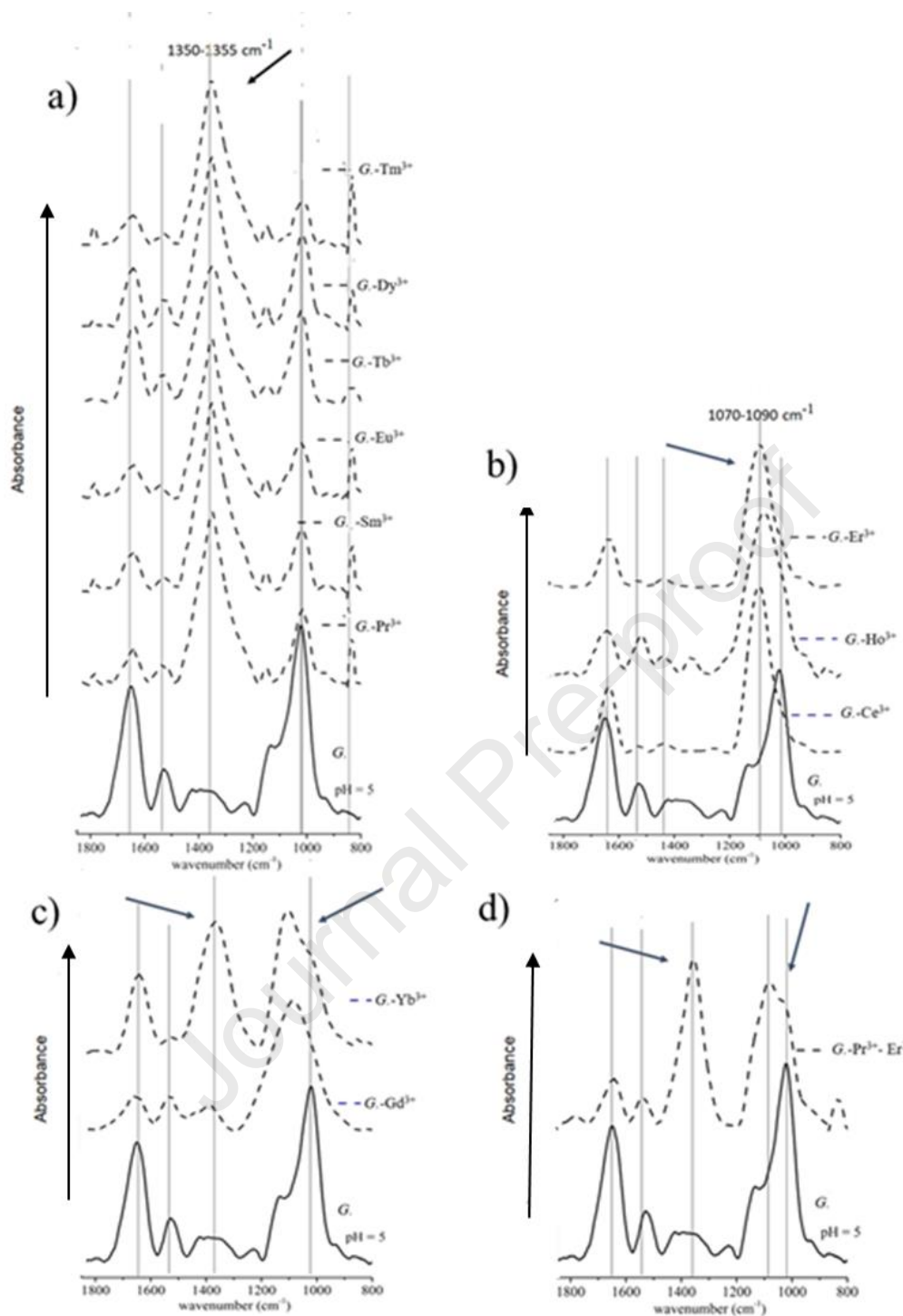
290
 291 Figure 2: a) pH(μF) experimental data (symbols) collected and fitting curves (dashed
 292 lines) obtained by using acid constants of Table 2, for the *G. sulphuraria* suspensions; b)
 293 ATR infrared absorbance spectra, in the 1850-800 cm^{-1} region, of dried *G. sulphuraria*
 294 suspensions at different pH values.
 295

296 The characterization of the acid-base properties of the *G. sulphuraria* was preliminary to
 297 investigation on her Lanthanides adsorptive ability.
 298

299 3.2 Lanthanides biosorption onto *G. sulphuraria*

300 3.2.1 FTIR-ATR and SEM-EDS characterization

301
 302 FTIR-ATR spectra were also recorded to highlight spectral features of *G. sulphuraria*
 303 surface after contact with lanthanides solutions.
 304



305

306

307

308

309

310

Figure 3: ATR infrared absorbance spectra, in the 1850–800 cm^{-1} region, of dried *G. sulphuraria* (lines) and *G. sulphuraria*- Ln^{3+} (dashed lines) suspensions at $\text{pH} \approx 5$. Changes in position and intensity of specific bands (1020 cm^{-1} and 1350 cm^{-1}) are highlighted by arrows.

311

In Figure 3 experimental FTIR-ATR spectra, in 1850–800 cm^{-1} region, of dried *G.*

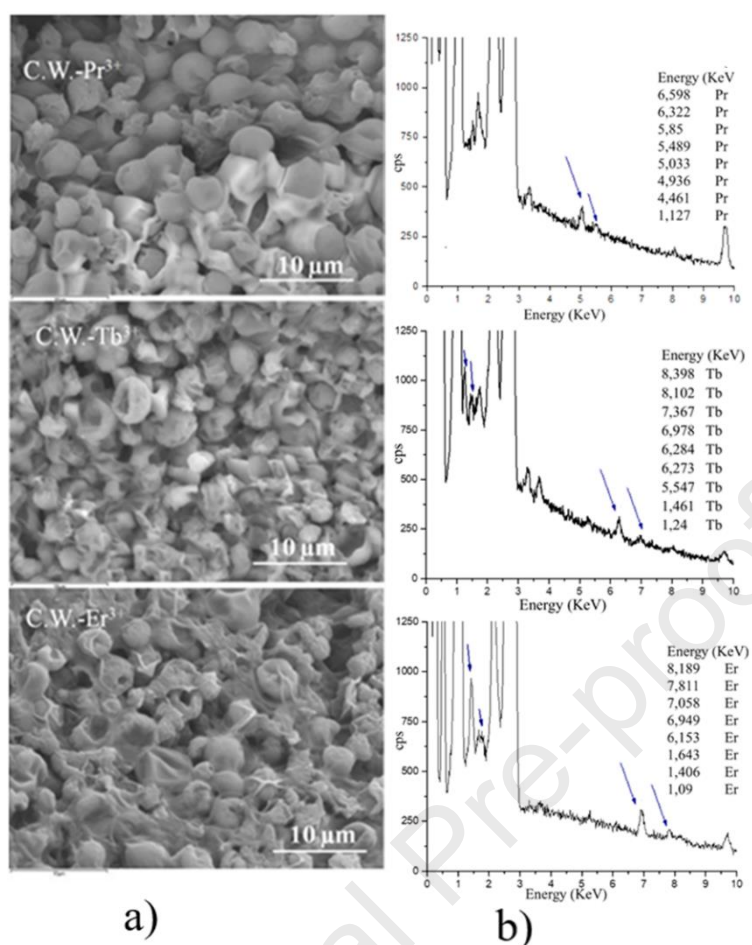
312

sulphuraria and *G. sulphuraria*- Ln^{3+} suspensions ($\text{pH} \approx 5$), are compared. Remarkable

313

changes in position and intensity of specific bands, in response to equimolar Ln^{3+}

314 solutions ($\text{Ln}^{3+} = \text{Ce}^{3+}, \text{Pr}^{3+}, \text{Sm}^{3+}, \text{Eu}^{3+}, \text{Gd}^{3+}, \text{Tb}^{3+}, \text{Dy}^{3+}, \text{Ho}^{3+}, \text{Er}^{3+}, \text{Tm}^{3+}, \text{Yb}^{3+}$), were
315 detected. More specifically, changes were remarked in the 1000 -1100 and 1340 -1360
316 cm^{-1} regions: the band at 1020 cm^{-1} (assigned to the C-O-C bending of carbohydrates
317 and/or polysaccharides) was shifted to a higher wavenumber, thus highlighting
318 interactions of the functional group with metal ion, if $\text{Ln}^{3+} = \text{Ce}^{3+}, \text{Ho}^{3+}, \text{Er}^{3+}$. In this
319 context, it is reported in literature that Er^{3+} complexes with carbohydrates. Moreover, the
320 extent of the displacement and the intensity of the band also seem to depend on the
321 amount of metal bound to the surface, as well as on the strength of complexation bond
322 (Yang et al., 2003). A sharp increase in the peak intensity at 1340-1360 cm^{-1} region
323 (assigned to protein), if $\text{Ln}^{3+} = \text{Pr}^{3+}, \text{Sm}^{3+}, \text{Eu}^{3+}, \text{Tb}^{3+}, \text{Dy}^{3+}, \text{Tm}^{3+}$, was also detected.
324 Finally, both regions of the spectrum appear modified if $\text{Ln}^{3+} = \text{Gd}^{3+}$ or Yb^{3+} highlighting
325 for the two lanthanides the ability to interact with both protein and carbohydrates.
326 Figure 3d shows the experimental spectrum of dried *G. sulphuraria*- Er^{3+} - Pr^{3+}
327 suspensions (mixture with $[\text{Pr}^{3+}]/[\text{Er}^{3+}] = 1$): two bands, at 1090 e 1355 cm^{-1} , were
328 detected, respectively. ATR-FTIR measurements highlight the suitability of functional
329 groups on *G. sulphuraria* surface to selectively sorption of Lanthanides ions.
330 SEM-EDS analysis of dried *G. sulphuraria* - Ln^{3+} suspensions ($\text{pH} \approx 5$, $\text{Ln}^{3+} = \text{Pr}^{3+}, \text{Tb}^{3+},$
331 Er^{3+}) were performed. Figure 4 shows high magnification SEM images (left) and related
332 EDS spectra (right). For the latter, the arrows highlight the characteristic peaks of the
333 lanthanides, whose ionization energy values are also reported to highlight their presence,
334 as also demonstrated by the previous tests. The results suggested that the solid particles,
335 after contact with Ln^{3+} , preserved their hollow aspect, as for the ones barely dispersed in
336 the NaCl medium, and it was not highlighted a significant variation in the aspect ratio.



337

338

339

340

341

342

343

344

345

346

347

348

349

350

351

352

Figure 4: a) High magnification SEM images (magnification 5000x) of dried *G. sulphuraria* - Ln³⁺ suspensions, in 0.5 M NaCl (pH ≈ 5, Ln³⁺ = Pr³⁺, Tb³⁺, Er³⁺). b) EDS spectra (magnification 100x): arrows show the characteristic peaks of the lanthanides, whose ionization energy values are also showed.

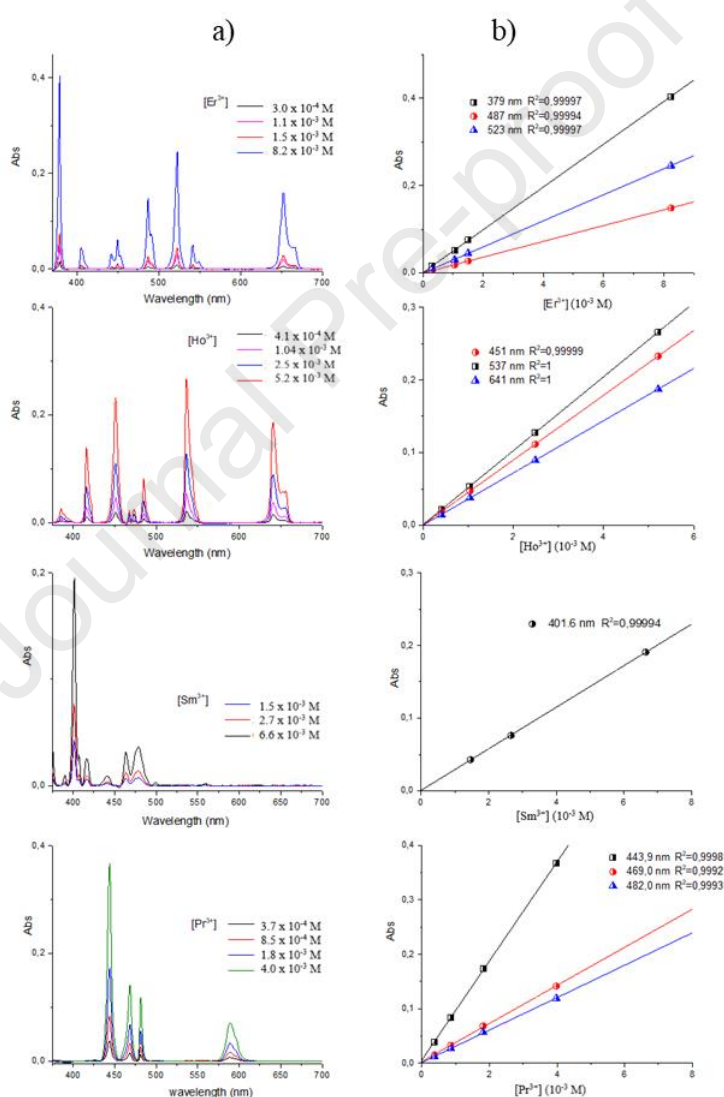
3.2.2 Biosorption experiments

Batch biosorption experiments were performed. The amount of Ln³⁺ on the *G. sulphuraria* surface, q , expressed as μmol/g (dry weight), was evaluated from the difference between analytical (total) concentration of metal ion, B , and the concentration of free ion, b , at equilibrium with metal ion onto *G. sulphuraria* surface, as follows:

$$q = \frac{V(B-b)}{m} \quad (6)$$

353 where V is the volume of the suspension, m is the mass (dry weight) of *G. sulphuraria*,
 354 respectively. The concentrations of free metal ions, b , were evaluated by UV-Vis
 355 spectrophotometry (if $\text{Ln}^{3+} = \text{Pr}^{3+}, \text{Sm}^{3+}, \text{Ho}^{3+}, \text{Er}^{3+}$) or ICP-MS using the external
 356 calibration (or standard addition) method. The UV-Vis spectra recorded in this work and
 357 Beer-Lambert's plot (Absorbance vs concentrations (M)) for Praseodymium, Samarium,
 358 Holmium, Erbium chloride stock solutions are show in the Figure 5.

359



360

361 Figure 5: a) Absorbance vs wavelength (nm) and b) Beer-Lambert's plot (Absorbance vs
 362 concentrations) for Praseodymium, Samarium, Holmium, Erbium chloride stock
 363 solutions.

364

365

366
367
368

Table 2: Experimental amount of Ln^{3+} biosorpted on the *G. sulphuraria* surface, q , expressed as $\mu\text{mol/g}$ (dry weight). The uncertainties (indicated in parenthesis) are to be intended as 3σ .

Pr^{3+} q ($\mu\text{mol/g}$)	Sm^{3+} q ($\mu\text{mol/g}$)	Eu^{3+} q ($\mu\text{mol/g}$)	Gd^{3+} * q ($\mu\text{mol/g}$)	Ho^{3+} q ($\mu\text{mol/g}$)	Er^{3+} q ($\mu\text{mol/g}$)	Tm^{3+} q ($\mu\text{mol/g}$)
140 ± 14 (pH =5)	120 ± 12 (pH =4.5)	140 ± 14 (pH =5)	80 ± 8 (pH =4)	80 ± 8 4 < pH < 5	80 ± 8 4 < pH < 5	110 ± 10 (pH =5)
80 ± 8 (pH =3.8)		80 ± 10 (pH =3.8)				

369
370

The experimental amount of Ln^{3+} biosorpted on the *G. sulphuraria* surface, q , reported in Table 2, highlighted the pH dependency of lanthanides biosorption onto *Galdieria*.

371

372

Desorption experiments showed the recovery efficiency of more than 90% if $\text{pH} < 1$.

373

374

Acid-base potentiometric-coulometric titrations of *G. sulphuraria*- Pr^{3+} suspensions, in 0.5 M NaCl, at 25.00 ± 0.03 °C, were performed. The reversibility was ensured throughout the pH range 3-7, investigated. The lower limit of acidity was chosen to avoid the precipitation of scarcely soluble oxide of metal ions (Baes and Mesmer, 1977; Biedermann and Sillen, 1953; Ferri et al., 2002; Vasca et al., 2004). The potentiometric data collected were interpreted by using a SCM approach (Wen et al. 1998; Schindler 1991; Wang and Giammar 2013; Kelly et al. 2002; David Borrok et al. 2004; Borrok and Fein 2004).

375

376

377

378

379

380

381

In the Figure 6a, the experimental data (pH/ μF), collected during titrations of *G. sulphuraria* and *G. sulphuraria*- Pr^{3+} suspensions, respectively, are compared. The potentiometric data have been interpreted by assuming complexation reaction of Eq. (7), with conditional equilibrium constant of Eq. (8). A good fit of the experimental data (dashed curves in Figure 6a) was obtained.

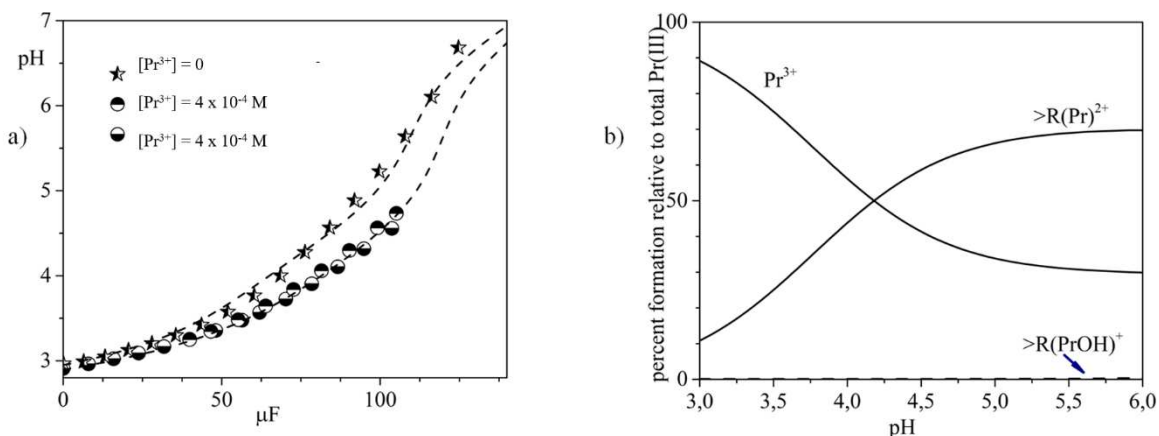
382

383

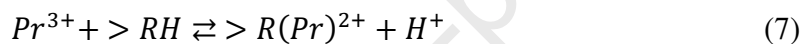
384

385

386



387
 388 Figure 6: a) pH(μF) experimental data (symbols) and fitting curves (dashed lines) collected
 389 for *G. sulphuraria* and *G. sulphuraria-Pr*³⁺ suspensions; b) Equilibrium distribution
 390 diagram of *G. sulphuraria-Pr*³⁺ system, in 0.5 M NaCl, constructed by equilibrium
 391 constants of Table 3.



$$393 \quad \beta = \frac{[>R(\text{Pr})^{2+}] \cdot [\text{H}^+]}{[>RH] \cdot [\text{Pr}^{3+}]} \quad (8)$$

394
 395
 396
 397 The brackets in the Eq. (8) represent the concentrations of the species in chemical
 398 equilibrium expressed in molarity. The equilibrium constants, β , calculated by numerical
 399 LETAGROP program (Sillen and Warnqvist, 1969), valid in 0.5 M NaCl, are reported in
 400 Table 3 and were used to construct the equilibrium distribution diagram (Hyperquad
 401 Simulation and Speciation, HySS 2009, program (Gans et al. 1996) of Figure 6b: the
 402 surface complexation with Pr^{3+} depends to pH and it appears remarkable at $\text{pH} > 4$.

403
 404 Table 3 Summary of the equilibrium constants, valid in 0.5 M NaCl, obtained in the
 405 present work, for the *G. sulphuraria-Pr*³⁺ system. The uncertainties (indicated in
 406 parenthesis) are to be intended as 3 σ .

Reaction	-Log β
$>R_1H + H_2O \rightleftharpoons >R_1^- + H_3O^+$	4.55(1)
$>R_2H + H_2O \rightleftharpoons >R_2^- + H_3O^+$	6.9(3)
$\text{Pr}^{3+} + >R_1H \rightleftharpoons >R_1(\text{Pr})^{2+} + \text{H}^+$	0.90(3)

408

409

410

411

412

413

414

415

416

417

418

419

420

421

422

423

424

425

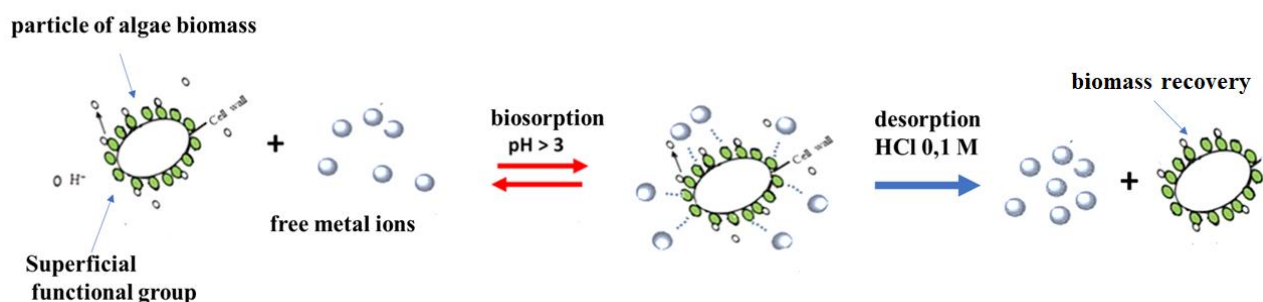
This paper describes a study concerning Ln^{3+} biosorption onto *G. sulphuraria*. A preliminary study to biosorption was the characterization of the acid-base properties of functional groups on *Galdieria* surface. As regards the biosorption, 11 trivalent lanthanides ions (Ce^{3+} , Pr^{3+} , Sm^{3+} , Eu^{3+} , Gd^{3+} , Tb^{3+} , Dy^{3+} , Yb^{3+}) have been considered. Furthermore, the desorption efficiency and the recovering the biosorbent to reuse it, have been also investigated. The study has been performed on *G. sulphuraria* lifeless cells to ensure a reproducibility of analytical results.

SEM-EDS, FTIR-ATR spectrometry, UV-Vis spectrophotometry and potentiometry techniques have been used. A pH-dependent biosorption behaviour, based on surface equilibrium reactions (complexation reactions of lanthanides by functional groups on *Galdieria* surface), with greater adsorption in the $5 < \text{pH} < 6$ range, was highlighted.

The lanthanides adsorbed can be easily recovered (90% removal rate) from acid solutions at $\text{pH} < 1$, and the biosorbent can be reused (not possible if *Galdieria* living cells are used).

For the Ln^{3+} biosorption-desorption onto *G. sulphuraria* surface, a mechanism based on a surface complexation model, was suggested, as also illustrated in Scheme 1.

Scheme 1: Mechanism for the Ln^{3+} biosorption-desorption on the *G. sulphuraria* surface.



426

427

428

429

430

The study suggests that *G. sulphuraria* could be used for the removing of trivalent actinides from aqueous solutions. The Ln^{3+} ions are used as models for trivalent actinides,

431 similar chemical elements to lanthanides (Baes and Mesmer, 1977; Biedermann and
432 Sillen, 1953; Ferri et al., 2002; Vasca et al., 2004), but too radioactive to be investigated
433 directly.

434

435 **4. Conclusions**

436

437 This paper describes a study concerned the use of *G. sulphuraria* lifeless cells as a
438 biosorbent for recovering Ln^{3+} from aqueous solutions. Particularly, the interaction ability
439 of *G. sulphuraria* with Ce^{3+} , Pr^{3+} , Sm^{3+} , Eu^{3+} , Gd^{3+} , Tb^{3+} , Dy^{3+} , Yb^{3+} , was investigated.
440 Biosorption is a cost-effective method for removing metal ions from aqueous solutions
441 and if biosorbent material have structural stability at higher acidity, the latter can be also
442 recycled. In this scenario, *G. sulphuraria*, a red alga thriving in geothermal sites with
443 peculiar ecological conditions (*i.e.*, low pH (0.5-3.0), $T \approx 50^\circ\text{C}$ - 55°C), is one of the best
444 candidates for the biological recovery of metals.

445 *G. sulphuraria* lifeless cells constitute a good biosorbent to removing Ln^{3+} from aqueous
446 solutions: a greater biosorption in the pH range $5 < \text{pH} < 6$ can be gained (ranging from 80
447 $\mu\text{mol/g}$ to 130 $\mu\text{mol/g}$); the adsorbed Ln^{3+} ions can be recovered at $\text{pH} < 1$ and, thus, the
448 biosorbent can be reused.

449 The study highlighted, also, that the lanthanides biosorption onto *Galdieria* involves
450 specific interactions between Ln^{3+} and functional groups onto surface: praseodymium,
451 samarium, europium, dysprosium, terbium and thulium form bonds with proteins groups;
452 cerium, erbium, and holmium interact with carbohydrates groups. This specificity in the
453 mechanism of Ln^{3+} biosorption onto *G. sulphuraria* (not described in literature) is
454 surprising considering the systematic and stepwise variation of the chemical and physical
455 properties of Lanthanides along the series, making difficult their separation. Furthermore,
456 this study could be of great applicative utility for the trivalent actinides biosorption from

457 waste aqueous solutions. Trivalent lanthanides are used to simulate the trivalent actinides.
458 In fact the chemical behaviour of actinides, that are strongly radioactive, is similar to that
459 of lanthanides in the same oxidation state.

460

461

462

463 **5. Acknowledgements**

464 We wish to express our gratitude and appreciation to Professor A.Squillace of
465 University Federico II of Naples for helpful discussions, support and assistance,
466 particularly, in SEM-EDS data collected.

467

6. Fundings

468

469

470

This research did not receive any specific grant from funding agencies in the public,
commercial, or not-for-profit sectors.

471

472 **Declaration of Competing Interest**

473

474

475

476

The authors declare that they have no known competing financial interests or personal
relationships that could have appeared to influence the work reported in this paper. **Author
contributions statement**

477

478

479

Conceptualization: C.M., C.C; **Methodology:** C.M. **Data curation:** C.M., A.EH;
Resources: M.T., M.I, S.J.D, M.P., C.C, C.L.; **Investigation:** A.J.A, A. E.H; **Formal
analysis:** C.M; **Writing - Original Draft:** C.M C.C

480

481

482

All authors have read and agreed to the published version of the paper

483

References

- 484 Baes, C., Mesmer, R., 1977. The hydrolysis of Cations, in: *Verichte Der Bunsengesellschaft Fur Fisikalische*
485 *Chemie*. pp. 245–246.
- 486 Balaram, V., 2019. Rare earth elements: A review of applications, occurrence, exploration, analysis,
487 recycling, and environmental impact. *Geosci. Front.* 10, 1285–1303.
488 <https://doi.org/10.1016/J.gsf.2018.12.005>
- 489 Balassone, G., Manfredi, C., Vasca, E., Bianco, M., Boni, M., Di Nunzio, A., Lombardo, F., Mozzillo, R.,
490 Maino, A., Mormone, A., Mura, G., Trifuoggi, M., Mondillo, N., 2021. Recycling REEs from the waste
491 products of silius mine (SE Sardinia, Italy): a preliminary study. *Sustain.* 13(24),
492 14000. <https://doi.org/10.3390/su132414000>
- 493 Barone, R., De Napoli, L., Mayol, L., Paolucci, M., Volpe, M.G., D'Elia, L., Pollio, A., Guida, M.,
494 Gambino, E., Carraturo, F., Marra, R., Vinale, F., Woo, S.L., Lorito, M., 2020. Autotrophic and
495 Heterotrophic Growth Conditions Modify Biomolecule Production in the Microalga *Galdieria*
496 *sulphuraria* (Cyanidiophyceae, Rhodophyta). *Mar. Drugs* 18, 169. <https://doi.org/10.3390/md18030169>
- 497 Biedermann, G., Sillen, L., 1953. Study on the Hydrolysis of Metal Ions. IV. *Ark.kemi* 40, 425–440.
- 498 Borrok, D., Fein, J., 2004. Distribution of protons and Cd between bacterial surfaces and dissolved humic
499 substances determined through chemical equilibrium modelling. *Geochim. Cosmochim. Acta* 68, 3043–
500 3052. <https://doi.org/10.1016/j.gca.2004.02.007>
- 501 Borrok, D., Fein, J.B., Kulpa, C.F., 2004. Proton and Cd adsorption onto natural bacterial consortia: Testing
502 universal adsorption behavior. *Geochim. Cosmochim. Acta* 68, 3231–3238.
503 <https://doi.org/10.1016/j.gca.2004.02.003>
- 504 Chakhmouradian, A.R., Wall, F., 2012. Rare earth elements: Minerals, mines, magnets (and more). *Elements*
505 8, 333–340. <https://doi.org/10.2113/gselements.8.5.333>
- 506 Ciniglia, C., Yang, E.C., Pollio, A., Pinto, G., Iovinella, M., Vitale, L., Yoon, H.S., 2014. Cyanidiophyceae
507 in Iceland: plastid *rbc L* gene elucidates origin and dispersal of extremophilic *Galdieria sulphuraria* and
508 *G. maxima* (Galdieriaceae, Rhodophyta). *Phycologia* 53, 542–551. <https://doi.org/10.2216/14-032.1>
- 509 Davis, J. A. and Kent, D. B. (1990). "Surface Complexation Modeling in Aqueous Geochemistry". *Mineral-*
510 *Water Interface Geochemistry, Reviews in Mineralogy Vol. 22*; Hochella, M. F. and White, A. F (eds)
511 Mineralogical Society of America.
- 512 Eren, A., Iovinella, M., Yoon, H.S., Cennamo, P., de Stefano, M., de Castro, O., Ciniglia, C., 2018. Genetic
513 structure of *Galdieria* populations from Iceland. *Polar Biol.* 41, 1681–1691.
514 <https://doi.org/10.1007/s00300-018-2308-3>
- 515 Ferri, D., Manfredi, C., Vasca, E., Fontanella, C., Caruso, V., 2002. Modelling of Natural Fluids: are the
516 available databases adequate for this purpose, in: A. Gianguzza (Ed.), *Chemistry of Marine Water and*
517 *Environmental Science Series, Part of: Environmental Science Series*, Springer-Verlag, New York,
518 2002, pp. 295–305 Chap. 12. <https://doi.org/10.1007/978-3-662-04935-8>.
- 519 Fu, F., Wang, Q., 2011. Removal of heavy metal ions from wastewaters: A review. *J. Environ. Manage.* 92,
520 407–418. <https://doi.org/10.1016/j.jenvman.2010.11.011>
- 521 Fukuda, S. ya, Yamamoto, R., Iwamoto, K., Minoda, A., 2018. Cellular accumulation of cesium in the
522 unicellular red alga *Galdieria sulphuraria* under mixotrophic conditions. *J. Appl. Phycol.* 30, 3057–
523 3061. <https://doi.org/10.1007/s10811-018-1525-z>
- 524 Gans, P., Sabatini, A., Vacca, A., 1996. Investigation of equilibria in solution Determination of
525 equilibrium constants with the HYPERQUAD suite programs, *Talanta* 43 1739–1753,
526 [https://doi.org/10.1016/0039-9140\(96\),01958-3](https://doi.org/10.1016/0039-9140(96),01958-3)
- 527 Goodenough, K.M., Schilling, J., Jonsson, E., Kalvig, P., Charles, N., Tuduri, J., Deady, E.A., Sadeghi, M.,
23

- 528 Schiellerup, H., Müller, A., Bertrand, G., Arvanitidis, N., Eliopoulos, D.G., Shaw, R.A., Thrane, K.,
529 Keulen, N., 2016. Europe's rare earth element resource potential: An overview of REE metallogenetic
530 provinces and their geodynamic setting. *Ore Geol. Rev.* 72, 838–856.
531 <https://doi.org/10.1016/j.oregeorev.2015.09.019>
- 532 Gran, G., 1952. Determination of the equivalence point in potentiometric acid-base titrations.
533 *Analyst* 77, 661–671. <https://doi.org/10.1039/AN9527700661>
- 534 Grenthe, I., 2002. Equilibrium Analysis, the Ionic Medium Method and Activity Factors, in: A.
535 Gianguzza (Ed.), *Chemistry of Marine Water and Environmental Science Series, Part of:*
536 *Environmental Science Series*, Springer-Verlag, New York, 2002, pp. 263–282 Chap. 10.
537 <https://doi.org/10.1007/978-3-662-04935-8>.
- 538 Gupta, C.K. and Krishnamurthy, N. (2005) *Extractive Metallurgy of Rare Earths*. CRC Press, Boca Radon.
- 539 Hu, Y., Florek, J., Larivière, D., Fontaine, F.G., Kleitz, F., 2018. Recent advances in the separation of rare
540 earth elements using mesoporous hybrid materials. *Chem. Rec.* 18, 1261–1276.
541 <https://doi.org/10.1002/tcr.201800012>
- 542 Huang, CP., Stumm, W. Spezifische, 1976. Adsorption von Kationen an wasserhaltiges γ -Al₂O₃. *Colloid &*
543 *Polymer Sci* **254**, 746. <https://doi.org/10.1007/BF01643779>
- 544 Iovinella, M., Lombardo, F., Ciniglia, C., Palmieri, M., di Cicco, M.R., Trifuoggi, M., Race, M., Manfredi,
545 C., Lubritto, C., Fabbicino, M., De Stefano, M., Davis, S.J., 2022. Bioremoval of Yttrium (III), Cerium
546 (III), Europium (III), and Terbium (III) from Single and Quaternary Aqueous Solutions Using the
547 Extremophile *Galdieria sulphuraria* (Galdieriaceae, Rhodophyta). *Plants* 11, 1376.
548 <https://doi.org/10.3390/plants11101376>
- 549 Ju, X., Igarashi, K., Miyashita, S. ichi, Mitsuhashi, H., Inagaki, K., Fujii, S. ichiro, Sawada, H., Kuwabara,
550 T., Minoda, A., 2016. Effective and selective recovery of gold and palladium ions from metal
551 wastewater using a sulfothermophilic red alga, *Galdieria sulphuraria*. *Bioresour. Technol.* 211, 759–
552 764. <https://doi.org/10.1016/j.biortech.2016.01.061>
- 553 Kelly, S.D., Kemner, K.M., Fein, J.B., Fowle, D.A., Boyanov, M.I., Bunker, B.A., Yee, N., 2002. X-ray
554 absorption fine structure determination of pH-dependent U-bacterial cell wall interactions. *Geochim.*
555 *Cosmochim. Acta* 66, 3855–3871. [https://doi.org/10.1016/S0016-7037\(02\)00947-X](https://doi.org/10.1016/S0016-7037(02)00947-X)
- 556 Kolodynska, D., Fila, D., Gajda, B., Gega, J., Hubicki, Z., 2019. Rare earth elements - separation methods
557 yesterday and today, in: Inamuddin, Ahamed, M., Asiri, A. (eds) *Applications of Ion Exchange*
558 *Materials in the Environment*. Springer, Cham., 161–185.
559 https://doi.org/10.1007/978-3-030-10430-6_8
560
- 561 Manfredi, C., Mozzillo, R., Volino, S., Trifuoggi, M., Giarra, A., Gargiulo, V., Alfé, M., 2020. On the
562 modeling of heavy metals and rare earth elements adsorption on colloidal carbon-based nanoparticles.
563 *Appl. Surf. Sci.* 505. <https://doi.org/10.1016/j.apsusc.2019.144264>
- 564 Mehta, R., Singhal, P., Singh, H., Damle, D., Sharma, A.K., 2016. Insight into thermophiles and their wide-
565 spectrum applications. *3 Biotech.* <https://doi.org/10.1007/s13205-016-0368-z>
- 566 Michalak, I., Chojnacka, K., Witek-Krowiak, A., 2013. State of the art for the biosorption process - A
567 review. *Appl. Biochem. Biotechnol.* 170, 1389–1416. <https://doi.org/10.1007/S12010-013-0269-0>
- 568 Minoda, A., Sawada, H., Suzuki, S., Miyashita, S. ichi, Inagaki, K., Yamamoto, T., Tsuzuki, M., 2015.
569 Recovery of rare earth elements from the sulfothermophilic red alga *Galdieria sulphuraria* using
570 aqueous acid. *Appl. Microbiol. Biotechnol.* 99, 1513–1519. <https://doi.org/10.1007/s00253-014-6070-3>
- 571 Schindler, P.W., 1991. A solution chemists view of surface chemistry. *Pure Appl. Chem.* 63, 1697–1704.
572 <https://doi.org/10.1351/pac199163121697>
- 573 Sillen, L., Warnqvist, B., 1969. High-speed computers as a supplement to graphical methods. VI. A strategy

- 574 for two-level LETAGROP adjustment of common and “group” parameters. Some features that avoid
575 divergence. *Ark.kemi* 31, 315–339.
- 576 Sirakov, M., Palmieri, M., Iovinella, M., Davis, S.J., Petriccione, M., di Cicco, M.R., De Stefano, M.,
577 Ciniglia, C., 2021. Cyanidiophyceae (Rhodophyta) Tolerance to Precious Metals: Metabolic Response
578 to Palladium and Gold. *Plants* 10, 2367. <https://doi.org/10.3390/plants10112367>
- 579 Stumm, W., Huang, C. P. and Jenkis, S. R., 1970. Specific Chemical Interactions Affecting the Stability of
580 Dispersed Systems, *Croat. Chem. Acta*, 42, 223-244.
- 581 Trifuoggi, M., Vasca, E., Manfredi, C., 2017. Rare earth elements equilibria in aqueous media, in: G.
582 Pagano (Ed.), *Rare Earth Elements in Human and Environmental Health at the Crossroads between*
583 *Toxicity and Safety*. Penthouse Level, Suntec Tower 3, 8 Temasek Boulevard, Singapore 038988 Pan
584 Stanford Publishing. Chapt. 11, 251–266.
- 585 Vasca, E., Ferri, D., Manfredi, C., Fantasma, F., Caruso, T., Fontanella, C., Vero, S., 2004. On the hydrolysis
586 of the Dysprosium(III) ion. *Chem. Speciat. Bioavailab.* 16, 71–77.
587 <https://doi.org/10.3184/095422904782775135>
- 588 Wall, F., 2014. Rare earth elements, in: *Critical Metal Handbook*. pp. 312–339.
- 589 Wang, Z., Giammar, D.E., 2013. Mass action expressions for bidentate adsorption in surface complexation
590 modeling: Theory and practice. *Environ. Sci. Technol.* 47, 3982–3996.
591 <https://doi.org/10.1021/es305180e>
- 592 Wen, X., Du, Q., Tang, H., 1998. Surface complexation model for the heavy metal adsorption on natural
593 sediment. *Environ. Sci. Technol.* 32, 870–875. <https://doi.org/10.1021/es970098q>
- 594 Xie, F., Zhang, T.A., Dreisinger, D., Doyle, F., 2014. A critical review on solvent extraction of rare earths
595 from aqueous solutions. *Miner. Eng.* 56, 10–28. <https://doi.org/10.1016/J.MINENG.2013.10.021>
- 596 Yang, L., Su, Y., Xu, Y., Wang, Z., Guo, Z., Weng, S., Yan, C., Zhang, S., Wu, J., 2003. Interactions
597 between metal ions and carbohydrates. Coordination, behaviour of neutral erythritol to Ca(II) and
598 lanthanide ions. *Inorg. chem* 42, 5844–5856.
- 599
- 600
- 601
- 602
- 603
- 604
- 605

Highlights

Lanthanides biosorption onto *G. sulphuraria* greater at pH > 4.

Specific interactions Lanthanides- functional groups onto *G. sulphuraria* surface.

Lanthanides biosorption mechanism onto *G. sulphuraria* explained by a Surface Complexation Model.

Journal Pre-proof

Declaration of interests

The authors declare that they have no known competing financial interests or personal relationships that could have appeared to influence the work reported in this paper.

The authors declare the following financial interests/personal relationships which may be considered as potential competing interests:

Journal Pre-proof